Investigations into Transition-State Geometry in the Mukaiyama Directed Aldol Reaction

Scott E. Denmark* and Wheeseong Lee[a]

Dedicated to Professor Teruaki Mukaiyama

Abstract: A model compound was designed to study the relative orientation of enol silane and carbonyl moieties in the Mukaiyama aldol reaction. The cyclization must proceed with either a synclinal or an antiperiplanar orientation of the aldehyde with respect to the enol silane. These two orientations lead to diastereomeric products, thus allowing for unambiguous correlation between product configuration and transition-state geometry. As steric bias is minimal, the product distribution should reflect the intrinsic preferences for reactant geometry in the transition state. Cyclizations of the model compound showed a modest preference for reaction via an antiperiplanar (open transition state) orientation of reactants in the presence of a wide range of Lewis acids (TiCl$_4$, SnCl$_4$, SnCl$_2$, BF$_3$·OEt$_2$, TMSBr, trityl perchlorate, EtAlCl$_2$) and triflic acid. The cyclizations promoted by tin(II) salts were *syn*-selective and dependent on the nature of the counterion. Fluoride ion promoted reactions were *anti*-selective and were independent of the nature of the cation.

Keywords: aldol reaction · fluorides · Lewis acids · stereoselectivity · transition states

Introduction

Of the many chemical legacies of Professor Teruaki Mukaiyama,[1] perhaps the most significant is his development of the directed aldol reaction that now bears his name.[2] The idea of using a preformed, stable enol derivative that could engage in additions to, for example, aldehydes and ketones was a brilliant solution to the problem of uncontrolled crossed aldolization.[3] This concept was the single most crucial advance that enabled the apotheosis of the aldol reaction to the stature it enjoys today as one of the most powerful and selective carbon–carbon bond-forming reactions.

The combination of an enoxysilane derivative of an aldehyde, ketone, ester, thioester, or other carbonyl compound with an aldehyde under the action of a Lewis acid is commonly known as the Mukaiyama directed aldol reaction.[4] This reaction can be activated by either Lewis acids or fluoride sources, and in some cases occurs without catalysts to produce up to four possible β-hydroxycarbonyl products after desilylation (Scheme 1). Enantioselective Mukaiyama
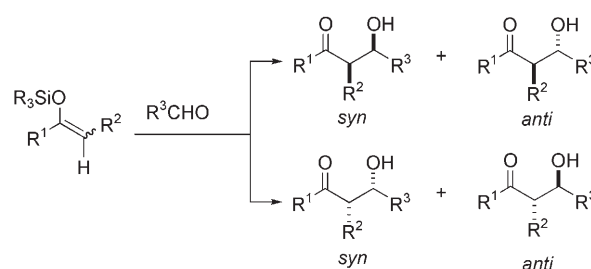
Scheme 1. Diastereomeric products from the Mukaiyama directed aldol reaction.

aldol reactions with chiral Lewis acids have been extensively developed over the past two decades.[5] Indeed, the number of reviews, books, monographs, and chapters summarizing the enormous literature on this transformation is fitting testimony to the impact of Professor Mukaiyama's inspirational studies.[6]

After a brief summary of the evolution of structure models of the transition state for the origin of stereocontrol in the Mukaiyama aldol addition, we will describe our stud-

[a] Prof. S. E. Denmark, W. Lee
Department of Chemistry
University of Illinois, Urbana
Illinois 61801 (USA)
Fax: (+217) 333-3984
E-mail: denmark@scs.uiuc.edu

ies on a model system designed to elucidate the existence of intrinsic stereoelectronic preferences in the carbon–carbon bond-forming event as well as the role of the Lewis acid. Studies on the stereochemical course of fluoride-promoted addition will also be described.

Background

Hypotheses for Transition-State Structures in Lewis Acid Induced Mukaiyama Aldol Reactions[7]
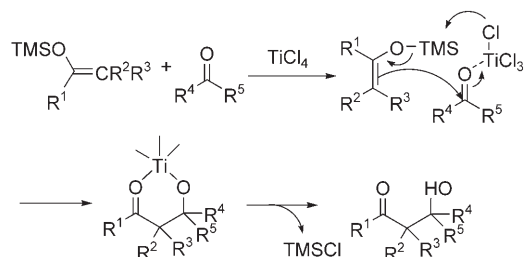
In their landmark report in 1973, Mukaiyama and co-workers described the first reaction of silyl enol ethers and aldehydes in the presence of stoichiometric amounts of titanium tetrachloride to afford β-hydroxyketones at room temperature.[2] The mechanistic pathway they proposed involved the formation of a titanium enolate after metal exchange (Scheme 2). The resulting titanium enolate was believed to react with an aldehyde to give a stable titanium aldolate. No structural evidence was supplied at the time.
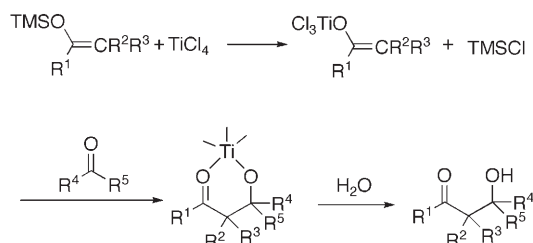
Scheme 2. Initial mechanistic hypothesis for the TiCl$_4$-promoted aldol addition. TMS = trimethylsilyl.

This first-proposed pathway was later revised by Mukaiyama et al. to a mechanism in which a metalloenolate is not involved (Scheme 3).[8] The absence of a metalloenolate was later unambiguously established by the use of an INEPT (insensitive nuclei enhanced by polarization transfer) ^{29}Si NMR spectroscopic study of the reaction between a silyl enol ether and a carbonyl compound.[9] Nevertheless, titanium (and presumably other) enolates can be prepared separately and can react with aldehydes with completely different stereochemical results (syn-selective) compared to the TiCl$_4$-induced reaction of silyl enol ethers (anti-selective).[10]

In the revised pathway, a Lewis acid is coordinated to the aldehyde oxygen atom. A large number of complexes between Lewis acids and carbonyl compounds have been thoroughly characterized by spectroscopic and crystallographic methods.[11] The complexation provides sufficient electrophilic activation to allow the enoxysilane derivative to add to the carbonyl group to afford the titanium-chelated aldolate and trimethylsilyl chloride (Scheme 3).

The diastereoselectivity was also investigated in the reaction of a silyl enol ether of cyclohexanone with benzaldehyde in the presence of TiCl$_4$, SnCl$_4$, or BF$_3$·OEt$_2$. There are no significant differences in diastereoselectivity between these three Lewis acids; all showed anti-enriched products with diastereomer ratios of 75:25, 76:24, and 74:26, respectively.

The first transition-state hypothesis to explain the syn/anti diastereoselectivity of Lewis acid mediated Mukaiyama reactions of silyl enol ethers and aldehydes was forwarded by Heathcock et al. in 1984.[12] Intermolecular reactions of various silyl enol ethers and aldehydes in the presence of representative Lewis acids were carried out (Scheme 4). For most
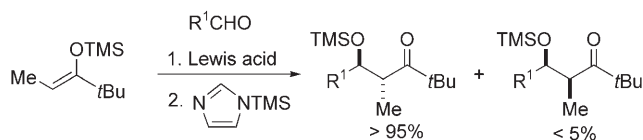
Scheme 4. anti-Selective addition of a bulky enoxysilane.

of the reactions examined, there was only modest stereoselectivity (syn/anti = 70:30–28:72). However, high anti selectivity (syn/anti < 5:95) was obtained in the reaction of the Z silyl enol ether of ethyl tert-butyl ketone with aldehydes in the presence of TiCl$_4$, SnCl$_4$, or BF$_3$·OEt$_2$.

Heathcock et al. postulated the involvement of open transition-state structures to explain the high anti selectivity of the Lewis acid mediated reaction of the Z silyl enol ether of ethyl tert-butyl ketone with benzaldehyde (Scheme 5).[12b] In these structures, the Lewis acid coordinates to the aldehyde oxygen atom in a position cis to the hydrogen atom to minimize steric repulsion.[12c] Transition-state structures T_1, T_2, and T_3 produce anti aldol adducts, whereas T_4, T_5, and T_6 afford syn products.

Synclinal transition-state structures T_3 and T_5 are disfavored because of the dipole–dipole interactions between the two carbon–oxygen bonds. T_3 is further destabilized by the nonbonding interactions between the phenyl and tert-butyl groups. T_4 is disfavored for the same reason. T_2 can be eliminated because of the interaction between the tert-butyl group and the Lewis acid. In T_6, there are severe interactions between the TMSO and phenyl groups as well as between the tert-butyl group and the carbonyl oxygen atom. Therefore, transition-state structure T_1 is the most favorable; the high anti selectivity is thus rationalized. When the tert-butyl group is replaced by a smaller group, the anti selectivity should decrease because of the increased contribution of transition-state structures T_4 and T_6. Indeed, with the

Scheme 3. Revised mechanism for the TiCl$_4$-promoted aldol addition.
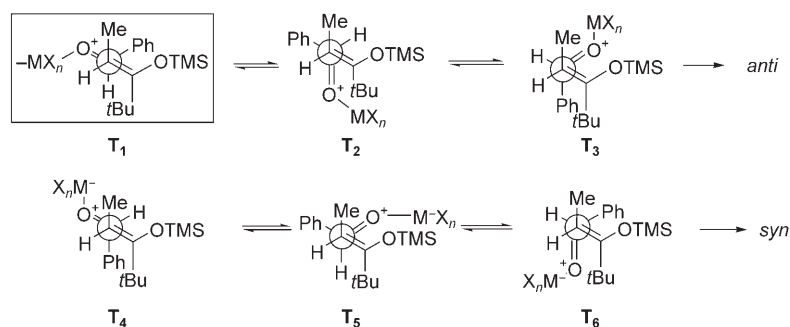
Scheme 5. The Heathcock analysis of transition-state structure.

silyl enol ether of diethyl ketone, the reaction showed modest *syn* selectivity (60:40).

Closed transition-state structures are excluded for the following three reasons. First, the lithium enolate of *tert*-butyl ethyl ketone reacts with high *syn* selectivity (*syn/anti* > 98:2), which is believed to arise from reaction via a closed transition-state structure.[13] Second, because the same selectivity is obtained with three different Lewis acids, BF3·OEt2, SnCl4, and TiCl4, no interactions seem to occur between the Lewis acid and the silyl group in the transition-state structures. Finally, Chan and Brook's investigations of the TiCl4-mediated reaction of bis(silyl ketene acetal)s with aldehydes established that the reactive intermediate is not a titanium enolate and that the coordination between TiCl4 and the silyloxy group is weak.[9a]

Aldol reactions of thiolester silyl ketene acetals with aldehydes showed enhanced *anti* selectivity (Scheme 6).[14] Furthermore, the high *anti* selectivity (*syn/anti* = 1:7–1:26) was obtained from either *E* or *Z* thiolester silyl ketene acetals. This convergent *anti* selectivity can be explained by "pinwheel" steric interactions.[15] For *E* thiolester silyl ketene acetals (Me is *Z* to the silyloxy group), transition-state structure T_7 is favored over T_8, which has interactions between the S*t*Bu and R^1 groups (the "pinwheel" interaction) as well
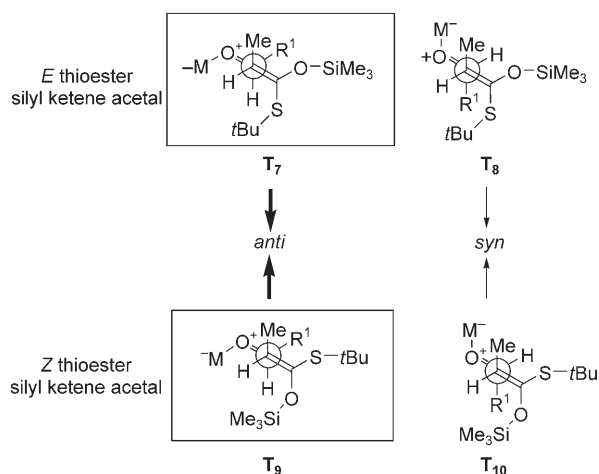
as between the Me group and the Lewis acid. For the *Z* thiolester silyl ketene acetal (Me is *trans* to the silyloxy group), transition-state structure T_{10} has interactions between the silyloxy group and R^1 (the "pinwheel" interaction) as well as between the Me group and the Lewis acid. The gauche interactions between the Me and R^1 groups in T_7 and T_9 are overwhelmed by the Lewis acid–Me interactions in T_8 and T_{10}. Therefore, the *anti* aldol selectivity is diastereoconvergent.

Mukaiyama et al. introduced the use of trityl salts as catalysts for the aldol reaction. In the presence of 5 mol% of trityl perchlorate, the *anti* aldol product was produced from both *E* and *Z* silyl enol ethers with *anti/syn* ratios of up to 84:16.[16] The diastereoselectivity is dependent on the substituents on silicon, and *anti* aldols always dominate from either *E* or *Z* silyl enol ethers. The open transition-state structures were proposed to explain the high *anti* selectivity and are independent of the geometry of silyl enol ethers (Scheme 7). For *E* silyl enol ethers, transition-state structure
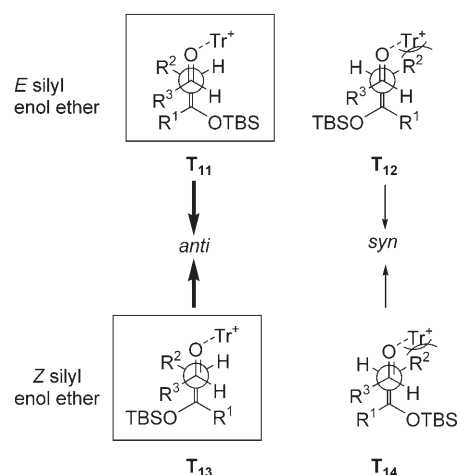
Scheme 7. Transition-state structures for trityl cation promoted aldol addition. TBS = *tert*-butyldimethylsilyl, Tr = trityl.

T_{11} is favored over T_{12} because the interaction between the large trityl group and R^2 in T_{12} is more severe than that between R^2 and R^3 in T_{11}. For the same reason, T_{13} is favored over T_{14} for *Z* silyl enol ethers.

Cyclic Transition-State Structures in Lewis Acid Induced Mukaiyama Reactions

Titanium tetrachloride catalyzed reactions of cyclic, cross-conjugated dienylsilyl ethers with aldehydes were investigated by Barner et al.[17] It was shown that the steric demand of the aldehyde plays a critical role in determining the stereoselectivity (Scheme 8). With pivalaldehyde, the *syn* adduct

Scheme 6. Transition-state structures for the addition of thiolester silyl ketene acetals.
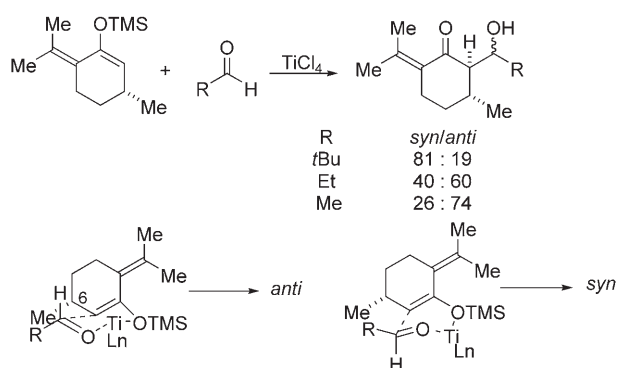
Scheme 8. Proposals for cyclic transition-state structures for TiCl$_4$-promoted aldol additions.

Scheme 9. Mechanistic pathways for fluoride-promoted aldol additions.

was formed preferentially (*syn/anti* = 81:19). With decreasing aldehyde size, *anti* adducts were enriched (albeit still the minor component) up to a *syn/anti* ratio of 74:26.

Six-membered, closed cyclic transition-state structures were proposed to explain the aldehyde-dependent selectivity (Scheme 8). The chairlike transition-state structure produces *anti* adducts, whereas the boatlike transition-state structure gives *syn* adducts. For small aldehydes (R = Me, Et), the reactions proceed via chairlike transition-state structures to afford *anti* products. As the size of R in the aldehyde increases (R = *t*Bu), the steric interaction between R and the substituent on C6 leads to a preference for a boat transition-state structure, thus rationalizing the formation of the *syn* product as the major isomer.

In recent years, Yamamoto and co-workers developed silver(I)–binap (binap = 2,2′-bis(diphenylphosphanyl)-1,1′-binaphthyl) catalysts for the enantioselective addition of stannyl and trimethoxysilyl enol ethers to aldehydes. They also speculated that the silver(I) ion serves to bridge the oxygen atoms of the reactive groups on the basis of the diastereodivergent selectivity with geometrically defined enol ethers.[18]

Fluoride-Induced Aldol Reactions of Silyl Enol Ethers

In 1976, Kuwajima and co-workers found that the fluoride ion can induce reactions between silyl enol ethers and aldehydes.[19] In the following year, Noyori et al. developed the fluoride-induced aldol reactions of silyl enol ethers and aldehydes.[20] In view of the high affinity of fluoride for silicon, two intermediates, the anionic pentacoordinate silicon species and the naked enolate, were proposed (Scheme 9).

In 1981, Noyori et al. reported that tris(diethylamino)sulfonium difluorotrimethylsiliconate (TASF) can also induce the reaction between a silyl enol ether and an aldehyde.[20b,c] A naked enolate with no interaction with the TAS countercation was proposed, and the reaction pathway is depicted
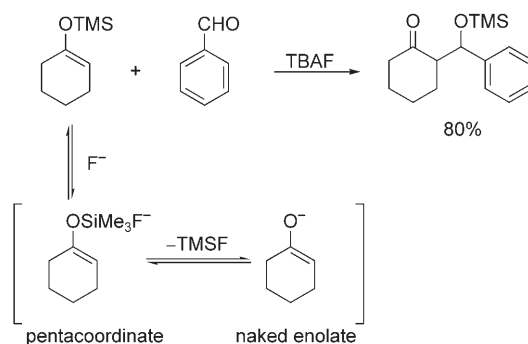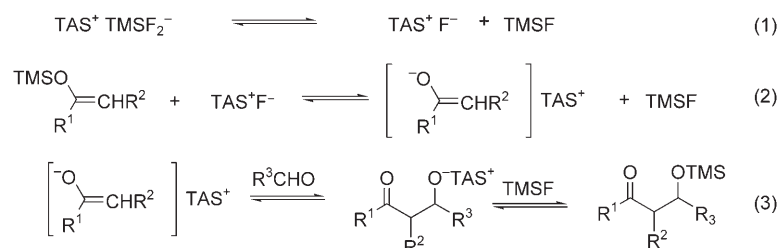
Scheme 10. Mechanistic interpretation of TASF-promoted additions.

in Scheme 10. On the basis of an NMR spectroscopic study, TAS$^+$TMSF$_2^-$ was considered to exist in equilibrium with TASF and TMSF [Eq. (1)]. The resulting fluoride reacts with the silyl enol ether to produce the TAS enolate [Eq. (2)]. After reaction with an aldehyde, TMSF traps the unstable aldolate [Eq. (3)].

Under conditions of kinetic control, *syn* aldol products were observed as the major isomers from either *E* or *Z* silyl enol ethers. To accommodate this behavior, new transition-state structures were proposed to explain the *syn* selectivity that is independent of enolate geometry (Scheme 11). The
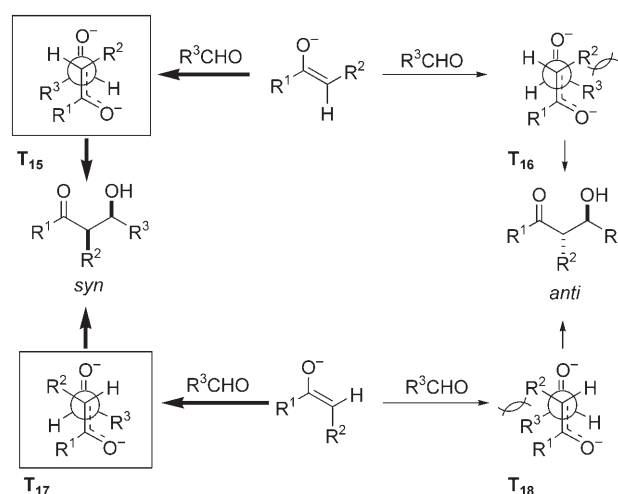
Scheme 11. Transition-state structures for aldol additions of "naked enolates".

electrostatic repulsion of the negatively charged oxygen atoms should be minimized in the extended transition-state structures. For Z enolates, transition-state structure T_{15} was believed t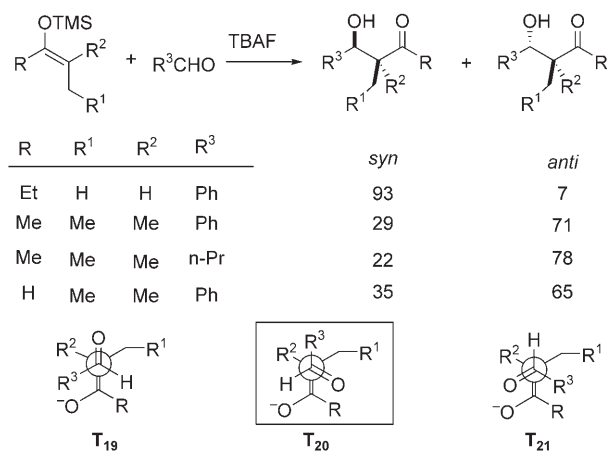o be favored over T_{16}, which has an R^2/R^3 interaction. Transition-state structure T_{17} from the E enolate was also believed to be favored over T_{18} for the same reason. Therefore, *syn* products are produced through T_{15} and T_{17} from Z and E silyl enol ethers, respectively.

Besides the "nonchelate, extended" transition-state structure, the "nonchelate, skew" transition-state structure was proposed to explain certain cases in fluoride-catalyzed aldol reactions of silyl enol ethers and aldehydes that afforded *anti* selectivity (Scheme 12).[19b] The hypothesis of the nonchelate, extended transition-state structure can explain the consistent selectivity upon variation of the counterion of the fluoride sources and the silyl groups. Furthermore, the same selectivity from different silyl groups, including trimethyl, dimethylphenyl, and triphenylsilyl derivatives, also remove the possibility of a pentacoordinate siliconate in the transition-state structures proposed by Corriu and co-workers.[21] However, the fluoride-induced reactions of tetra- or trisubstituted E silyl enol ethers with aldehydes were found to be *anti*-selective rather than the usual *syn*-selective in fluoride-induced reactions.

This *anti* selectivity cannot be rationalized by extended transition-state structures. Instead, the "nonchelate, skew" transition-state structures for *anti* products from the reaction of E silyl enol ethers with aldehydes was introduced (Scheme 12). Transition-state structure T_{19} has a gauche interaction between R^2 and R^3, and T_{20} has a dipole–dipole repulsion between the two carbon–oxygen bonds. Ab initio

calculations showed that T_{19} and T_{20} are of equally low energy, and T_{21} is disfavored by $3.3\ kcal\,mol^{-1}$ due to oxygen–oxygen repulsion.[19] Therefore, T_{20} should have a significant contribution in this reaction.
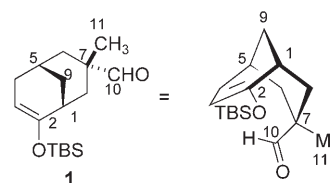
Hypervalent silyl enol ether mechanisms were proposed by Corriu and co-workers for the fluoride-mediated reaction of silyl enol ethers and aldehydes (Scheme 13).[21] Two competing pathways were believed to be dependent on the fluo-
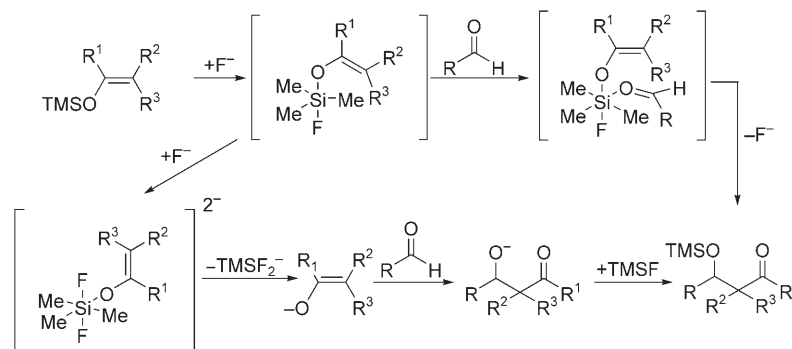
Scheme 13. The Corriu open and closed transition-state structures for fluoride-promoted aldol additions.

ride sources. After the association of the first fluoride ion, a common pentacoordinate silicon species is produced. In the case of very reactive fluoride sources (such as TASF or $R_4N^+F^-$), the fluoride ion attacks the pentacoordinate siliconate to produce a "naked enolate" by losing $TMSF_2^-$. The second mechanism involves a "hypervalent" silicon intermediate for less-reactive fluoride sources such as CsF or KF. In this case, the pentacoordinate siliconate is attacked by the aldehyde oxygen atom to afford a hexacoordinate silicon intermediate.

Although there are many reports about the reaction pathways and the transition-state structures in the aldol reactions of silyl enol ethers and aldehydes, the origin of stereogenesis and the elements that govern the steric course of the Mukaiyama aldol reactions are not well-understood. To address this concern, model system **1** was designed to investigate the transition-state geometry in the presence of Lewis acids and fluoride sources (Scheme 14).

Scheme 12. Alternative transition-state structures for aldol additions of "naked enolates".

R	R^1	R^2	R^3	*syn*	*anti*
Et	H	H	Ph	93	7
Me	Me	Me	Ph	29	71
Me	Me	Me	n-Pr	22	78
H	Me	Me	Ph	35	65

Scheme 14. Model system **1** for the investigation of the Mukaiyama aldol reaction.

Model system **1** embodies several features that are important for the investigation of transition-state structures in the Mukaiyama aldol reaction: 1) the intramolecular reaction removes the ambiguity of assigning the disposition of the re-

FULL PAPERS

actants in an intermolecular reaction, 2) steric bias is minimized by the nearly symmetrical nature of the starting silyl enol ether–aldehyde, and 3) the formation of an adamantane framework in aldol products ensures kinetic control.

In the Lewis acid induced cyclization of **1**, there are two limiting reactive geometries that are accessible from the rotation about the C7–formyl bond that correspond to the synclinal and antiperiplanar transition-state structures **T₂₂** and **T₂₃**, respectively (Scheme 15). The Lewis acid coordinates to the aldehyde oxygen atom in a position *syn* to the aldehyde hydrogen atom.[11] In the synclinal transition-state structure **T₂₂**, which affords the *syn* aldol product, there should be a steric interaction between the silyloxy group and the Lewis acid complex along with an unfavorable dipole repulsion between the two carbon–oxygen bonds. The antiperiplanar transition-state structure **T₂₃** is free from those interactions and produces the *anti* aldol product. Therefore, the ratio of the diastereomeric aldol products provides a measure of the synclinal/antiperiplanar preference for the corresponding transition-state structure. An antiperiplanar arrangement of the groups is currently the most popular formulation of the transition state and has been supported by an extensive

survey of additions by Heathcock et al.[12] and Gennari et al.[22]

Furthermore, model system **1** can be employed to examine the reaction pathway in fluoride ion induced aldol reactions. The two distinct pathways proposed by Corriu and co-workers[21] for a fluoride ion induced, nucleophilically activated reaction involving the hexacoordinate siliconate and the "naked" enolate can be probed by using **1**, because the two distinct pathways lead to different products (Scheme 16).

In transition-state structure **T₂₄**, the aldehyde oxygen atom is coordinated to silicon due to the enhanced Lewis acidity of silicon after being attacked by one fluoride ion.[23] This synclinal "hexacoordinate siliconate" transition-state structure should give the *syn* aldol product. For reactive fluoride sources, another fluoride ion attacks the silicon atom to give the difluorohexacoordinate siliconate. In this case, the aldehyde oxygen atom cannot coordinate to the silyl group; it loses difluorosiliconate to give the "naked enolate". Naked enolates produce *anti* aldols through the antiperiplanar transition-state structure **T₂₅** to reduce dipole–dipole repulsion between the two oxygen atoms.
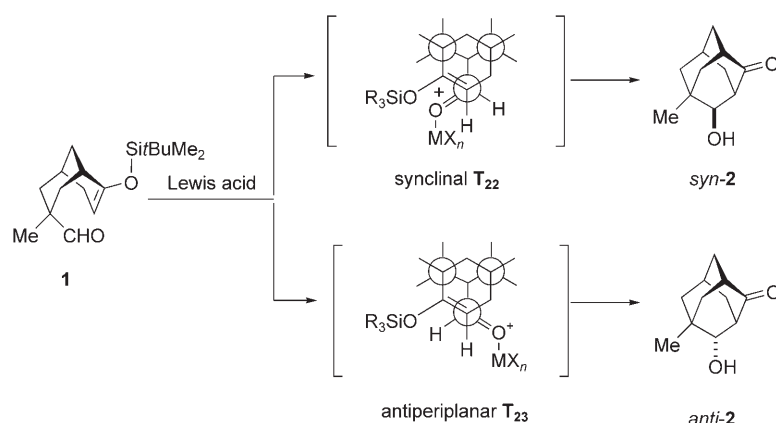
Scheme 15. Geometries of the transition-state structures for the cyclization of model **1** with Lewis acids.
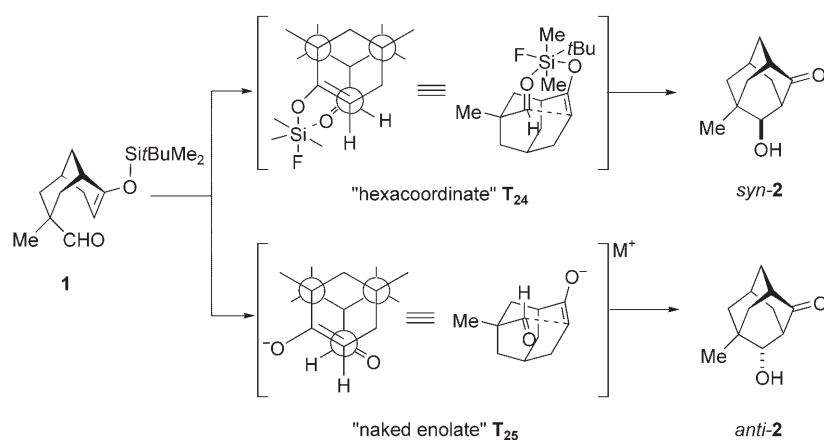
Scheme 16. Geometries of the transition-state structures for cyclization of model **1** with fluoride.

Results

Synthesis of Model System 1

The three strategies that were considered for the synthesis of model system **1** are 1) oxidation of an enoxysilane alcohol, 2) reduction of enoxysilane carboxy derivatives, and 3) deprotection of an enoxysilane-protected aldehyde (Scheme 17).

Oxidation of the alcohol to the corresponding aldehyde requires a strong oxidizing agent because of the neopentyl nature of the primary alcohol. Furthermore, the oxidation reactions must be performed under neutral or mildly basic conditions because the silyl enol ether is labile in an acidic environment. Although reducing agents generally do not react with silyl enol ethers, strong agents would be required for the reduction of tertiary and hindered carboxy derivatives. Finally, the route that involves protection of the aldehyde requires mildly basic deprotection conditions,
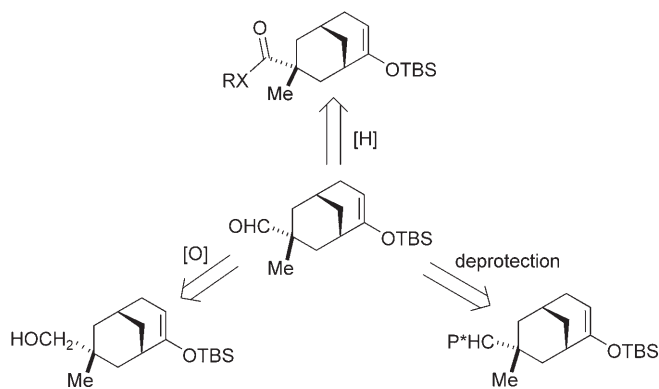
Scheme 17. Synthetic approaches for model **1**.

Scheme 18. Requirements for the protecting group P* in the synthesis of model **1**. Bz = benzoyl.

again because of the acid sensitivity of the silyl enol ether.

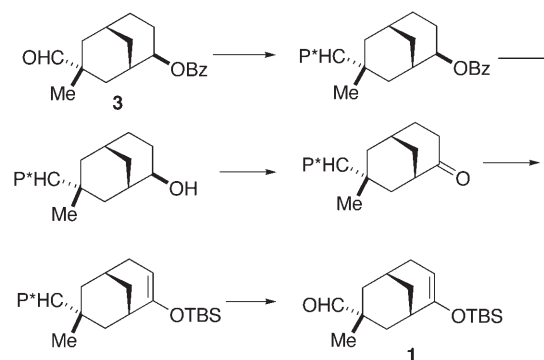Strategies that involve oxidation of alcohol–alcohol or reduction of carboxy–carboxy derivatives to the corresponding enoxysilane aldehyde failed despite considerable experimentation and variation of conditions. Ultimately, the successful strategy entailed protection of the aldehyde and deprotection after construction of the enoxysilane portion of the molecule (Scheme 18). However, this approach required the invention of a new protecting group (P*) for the aldehyde. This protecting group must be resistant to debenzoylation, oxidation, and enolization conditions. Furthermore, the protecting group must be removable under basic conditions so that the enoxysilane moiety can survive.

The protecting group designed for this purpose was a dioxolanone derived from α,α-dimethylisobutyric acid. A dioxolanone protecting group was selected for the following reasons: 1) the aldehyde can be protected under mild conditions, 2) the dioxolanone group should be resistant to oxidation conditions, 3) this group is not enolizable because of the two methyl substituents at the α carbon atom, and 4) this protecting group is removable under mildly basic conditions to give the corresponding aldehyde by hydrolysis of the lactone.

To facilitate installation of the protecting group, 2-hydroxyisobutyric acid was combined with 2 equivalents of TMSCl in the presence of Et₃N to give the bis-silylated hydroxy ester **4** (Scheme 19).[24] The synthesis of aldehyde **3** has already been detailed in the context of an earlier model system.[25] The protection of

the formyl group in **3** with **4** in the presence of TMSOTf and 2,6-DTBP gave 1,3-dioxolan-4-one **5** in 91% yield.[26] This intermediate is very stable and could be stored in the freezer for months. The next challenge was the removal of the benzoate protecting group in the presence of the dioxolanone group. Unfortunately, the latter is reactive toward deprotection reagents, and typical saponification methods returned benzoate aldehyde **3**. Potassium *tert*-butoxide also removed the dioxolanone group first, and methanol at reflux gave no reaction.

The successful removal of the benzoate group without loss of the dioxolanone moiety was ultimately accomplished by the use of 2.0 equivalents of DIBALH at low temperature. The mechanism of removal of the benzoyl group with DIBALH is depicted in Scheme 19. The first equivalent of DIBALH attacked the dioxolanone, and the resulting dioxo-
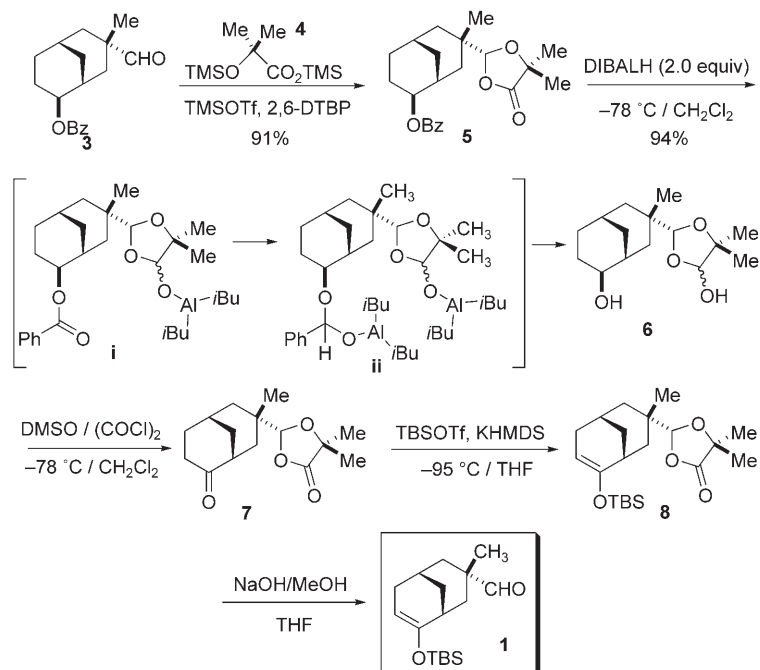
Scheme 19. Synthetic scheme for model **1**. DIBAL = diisobutylaluminum hydride, DMSO = dimethyl sulfoxide, 2,6-DTBP = 2,6-di-*tert*-butylpyridine, HMDS = 1,1,1,3,3,3-hexamethyldisilazane, Tf = trifluoromethanesulfonyl.

lanoxylaluminum intermediate **i** did not decompose to aldehyde **3** at −78 °C.[27] The second equivalent of DIBALH attacked the benzoyl group to give hydroxy dioxolanol **6**. Dioxolanol **6** was remarkably stable and could be recovered by silica-gel column chromatography in high yield (94 %).
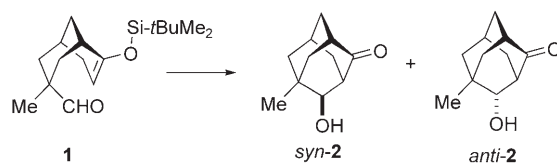
Oxidation of diol **6** with 2 equivalents of the Swern reagent[28] produced keto dioxolanone **7** in 88 % yield (Scheme 19). The solid **7** is a very stable intermediate and could be stored in the freezer for months without decomposition. Deprotonation of the ketone with KHMDS in the presence of TBSOTf at −95 °C cleanly afforded silyl enol ether dioxolanone **8** in 92 % yield. This reaction required very low temperature to prevent the resulting enolate from cyclizing. Instead, the potassium enolate was trapped by the TBSOTf that was present prior to the deprotonation. Careful workup was required because **8** is extremely sensitive to reaction. Under acidic conditions, the silyl enol ether group would be lost, whereas under basic conditions the dioxolanone group could be removed. A pH 9 buffer solution was used for workup. Hexane was used for extraction, because the product **8** decomposed upon evaporation when more-hydrophilic solvents were used. After the extracts were dried, enoxysilane dioxolanone **8** was purified by column chromatography on Activity III neutral alumina by using a jacketed column with circulating cold (−78 °C) acetone as a coolant. Silyl enol ether **8** cyclized upon purification at higher temperature or with alumina of higher activity.

The selective removal of the dioxolanone protective group without destroying the enoxysilane was the most important challenge in the synthesis of model system **1**. After many deprotection strategies were surveyed, it was successfully accomplished by treatment with 5 % NaOH in MeOH at 0 °C to produce the desired silyl enol ether aldehyde **1** in 83 % yield (Scheme 19). Methanol must be distilled from CaSO$_4$, not P$_2$O$_5$, to remove any possible acidic source, and the reaction must be quenched with pH 9 buffer at 0 °C. Very careful extraction and drying were required because **1** is extremely sensitive to hydrolysis with traces of water. Hexane (distilled from K$_2$CO$_3$) was used as the extracting solvent, and sodium sulfate was used to dry the extracts. The final product was purified by column chromatography at −78 °C on Activity V basic alumina. Model system **1** solidified in a freezer and was stable for 3–4 days without cyclization.

Cyclization Results from Model System 1

Cyclizations of **1** were carried out with a Lewis acid (1.1 equiv) in dry CH$_2$Cl$_2$ at −78 °C for 1 h followed by desilylation with 10 equiv of tetra-*n*-butylammonium fluoride (TBAF) at room temperature for 2–3 h. Analysis of the product ratio was carried out by capillary GC.[29] Control experiments with pure, silylated aldol products from *anti*-**2** or *syn*-**2** with the catalysts showed no cross-over; these reactions were thus demonstrated to be under kinetic control. Results of the cyclization of **1** with several representative Lewis acids and a fluoride ion source are summarized in Table 1.

Table 1. Representative Lewis acid and fluoride-induced aldol reactions of **1**.[a]

Entry	Lewis acid ([equiv])	Solvent	*t* [h]	*syn*-2/*anti*-2[b]	$\Delta\Delta G^{\neq}$ [kcal mol^{-1}]
1	TiCl$_4$ (1.1)	CH$_2$Cl$_2$	1	21:79	−0.51
2	SnCl$_4$ (1.1)	CH$_2$Cl$_2$	1	18:82	−0.59
3	EtAlCl$_2$ (1.1)	CH$_2$Cl$_2$	1	24:76	−0.45
4	BF$_3$·OEt$_2$ (1.1)	CH$_2$Cl$_2$	1	29:71	−0.35
5	TMSBr (1.1)	CH$_2$Cl$_2$	1	30:70	−0.33
6	TMSOTf (1.1)	CH$_2$Cl$_2$	1	25:75	−0.43
7	TrClO$_4$ (0.1)	CH$_2$Cl$_2$	1	27:73	−0.39
8	CF$_3$SO$_3$H (1.1)	CH$_2$Cl$_2$	1	18:82	−0.59
9	TBAF (1.1)	THF	24	18:82	−0.59

[a] All cyclizations were performed at −78 °C. [b] Determined by capillary GC analysis, average of at least three runs within ±3 %.

In general, the Lewis acid promoted reactions showed modest *anti* selectivity. Tetravalent Lewis acids TiCl$_4$ and SnCl$_4$ gave 21:79 and 18:82 *syn*/*anti* selectivity, respectively (Table 1, entries 1 and 2). Aluminum- and boron-type Lewis acids EtAlCl$_2$ and BF$_3$·OEt$_2$ also showed 24:76 and 29:71 *syn*/*anti* selectivity (Table 1, entries 3 and 4). Silicon-containing Lewis acids TMSBr and TMSOTf showed 30:70 and 25:75 *syn*/*anti* selectivity (Table 1, entries 5 and 6). In the case of trityl perchlorate, only a catalytic amount of Lewis acid was used, and the cyclization occurred with 27:73 *syn*/*anti* selectivity (Table 1, entry 7). The Brønsted acid CF$_3$SO$_3$H also displayed *anti* selectivity (Table 1, entry 8). Fluoride-induced cyclization with TBAF was slow; it took 24 h to complete in THF. This reaction also displayed *anti* selectivity, with a *syn*/*anti* ratio of 20:80 (Table 1, entry 9).

Given the wide range of Lewis acid types examined, the narrow range of selectivities was remarkable. Furthermore, the selectivities of all the Lewis acid induced cyclizations are very similar to that of TfOH. To exclude the possibility that these similar selectivities arose from catalysis by a common protic acid, the cyclizations of **1** were performed in the presence of 2,6-DTBP as an acid scavenger (Table 2). The TiCl$_4$-induced cyclization of **1** in the presence of 2,6-DTBP showed very little change in selectivity (Table 2, entry 1). Other Lewis acids such as EtAlCl$_2$, TMSOTf, and TrClO$_4$ also showed only minor changes in selectivity (Table 2, entries 3, 6, and 7). Thus, it was concluded that the similar *anti* selectivities of these Lewis acids did not arise from protic-acid catalysis. However, SnCl$_4$ showed an unexpected reversal in selectivity from 18:82 *anti* selective to 61:39 *syn* selective (Table 2, entry 2). The remarkable reversal in selectivity with SnCl$_4$ suggests that a protic-acid source existed in SnCl$_4$ and induced cyclization. Cyclization with TBAF in the presence of 2,6-DTBP showed no change in selectivity (Table 2, entry 9). From these results, it can be

Table 2. Lewis acid induced cyclizations of **1** without and with 2,6-di-*tert*-butylpyridine.[a]

Entry	Lewis acid ([equiv])	Solvent	t [h]	*syn*-**2**/ *anti*-**2**[b]	*syn*-**2**/ *anti*-**2**[b,c]	$\Delta\Delta G^{\ne[c]}$ [kcal mol^{-1}]
1	TiCl$_4$ (1.1)	CH$_2$Cl$_2$	1	21:79	25:75	−0.43
2	SnCl$_4$ (1.1)	CH$_2$Cl$_2$	1	18:82	61:39	0.17
3	EtAlCl$_2$ (1.1)	CH$_2$Cl$_2$	1	24:76	25:75	−0.43
4	BF$_3$·OEt$_2$ (1.1)	CH$_2$Cl$_2$	1	29:71	–	−0.35
5	TMSBr (1.1)	CH$_2$Cl$_2$	1	30:70	–	−0.33
6	TMSOTf (1.1)	CH$_2$Cl$_2$	1	25:75	27:73	−0.39
7	TrClO$_4$ (0.1)	CH$_2$Cl$_2$	1	27:73	28:72	−0.37
8	CF$_3$SO$_3$H (1.1)	CH$_2$Cl$_2$	1	18:82	–	−0.59
9	TBAF (1.1)	THF	24	20:80	19:81	−0.56

[a] All cyclizations were performed at −78 °C. [b] Determined by capillary GC analysis, average of at least three runs within ±3%. [c] Reaction in the presence of 2,6-di-*tert*-butylpyridine.

concluded that the *anti* selectivity was not the result of Brønsted acid catalysis, except in the case of SnCl$_4$.

Investigations with other Lewis acids are summarized in Table 3. In Table 3, entry 1, SiCl$_4$ showed less *anti* selectivity than TiCl$_4$. Diethylaluminum chloride showed almost the same selectivity as a monoalkylaluminum dichloride (Table 3, entry 2). No change in selectivity was observed between TBDMSOTf and TMSOTf (Table 3, entry 3). Two different trityl cation sources, TrBF$_4$ and TrOTf, showed similar selectivity (Table 3, entries 4 and 5). Trifluoroacetic acid showed less *anti* selectivity than TfOH (Table 3, entry 6). A mixed catalyst system of 0.08 equivalents of SnCl$_2$ and TMSCl showed almost the same selectivity as 0.05 equivalents of tin(II) chloride and TrCl (Table 3, entries 7 and 8). With 1.1 equivalents of both SnCl$_2$ and TrCl, an increase in *syn* selectivity was observed (Table 3, entry 9). Tributyltin fluoride showed slight *syn* selectivity; therefore, it did not seem to behave as a fluoride ion source but as a Lewis acid (Table 3, entry 10). The reaction did not go to completion in the presence of Ti(O*i*Pr)$_4$ (Table 3, entry 11). Reactions with

Table 3. Lewis acid induced cyclizations of **1** without and with 2,6-di-*tert*-butylpyridine.[a]

Entry	Lewis acid ([equiv])	*syn*-**2**/ *anti*-**2**[b]	*syn*-**2**/ *anti*-**2**[b,c]	$\Delta\Delta G^{\ne[c]}$ [kcal mol^{-1}]
1	SiCl$_4$ (1.1)	27:73	–	−0.39
2	Et$_2$AlCl (1.1)	28:72	–	−0.37
3	TBDMSOTf (1.1)	27:73	30:70	−0.39
4	TrBF$_4$ (0.1)	17:83	–	−0.61
5	TrOTf (0.1)	18:82	–	−0.59
6	CF$_3$CO$_2$H (1.1)	35:65	–	−0.24
7	SnCl$_2$+TMSCl (0.08)	45:55	–	−0.08
8	SnCl$_2$+TrCl (0.05)	43:57	–	−0.11
9	SnCl$_2$+TrCl (1.1)	62:38	–	0.19
10	Bu$_3$SnF (1.1)	46:54	53:47	0.05
11	Ti(O*i*Pr)$_4$ (1.1)	incomplete	–	–
12	LiClO$_4$ (1.1)	41:59	34:66	−0.26
13	SbCl$_3$ (1.1)	38:62	–	−0.19

[a] All cyclizations were performed in methylene chloride at −78 °C for 1 h. [b] Determined by capillary GC analysis, average of at least three runs within ±3%. [c] Reaction in the presence of 2,6-di-*tert*-butylpyridine.

LiClO$_4$ and SbCl$_3$ showed slight *anti* selectivity (Table 3, entries 12 and 13).

Further studies on the influence of solvent and stoichiometry on the selectivity effected by TiCl$_4$ and BF$_3$·OEt$_2$ were carried out, and the results are summarized in Table 4. A stoichiometry study with TiCl$_4$ (Table 4, entries 1–3) revealed no selectivity dependence on the amount of reagent. Table 4, entry 4 showed that TiCl$_4$-induced cyclization in

Table 4. Cyclizations of **1** with TiCl$_4$ and BF$_3$·OEt$_2$ under various conditions.[a]

Entry	Lewis acid ([equiv])	Solvent	*syn*-**2**/ *anti*-**2**[b]	*syn*-**2**/*anti*-**2**[b,c]	$\Delta\Delta G^{\ne[c]}$ [kcal mol^{-1}]
1	TiCl$_4$ (0.5)	CH$_2$Cl$_2$	20:80	–	−0.54
2	TiCl$_4$ (1.1)	CH$_2$Cl$_2$	21:79	25:75	−0.43
3	TiCl$_4$ (3)	CH$_2$Cl$_2$	21:79	–	−0.51
4	TiCl$_4$ (1.1)	THF	incomplete	–	–
5	BF$_3$·OEt$_2$ (0.5)	CH$_2$Cl$_2$	24:76	–	−0.45
6	BF$_3$·OEt$_2$ (1.1)	CH$_2$Cl$_2$	29:71	–	−0.35
7	BF$_3$·OEt$_2$ (3)	CH$_2$Cl$_2$	22:78	–	−0.49

[a] All cyclizations were performed at −78 °C for 1 h. [b] Determined by capillary GC analysis, average of at least three runs within ±3%. [c] Reaction in the presence of 2,6-di-*tert*-butylpyridine.

THF was not complete, most likely because TiCl$_4$ is strongly coordinated to THF. Finally, BF$_3$·OEt$_2$ showed similar *anti* selectivity that was not dependent on the stoichiometry of the reagents (Table 4, entries 5–7).

The results from a stoichiometry study with SnCl$_4$ and Sn^{II} Lewis acids are summarized in Table 5. The stoichiometry study with SnCl$_4$ showed *syn* selectivity independent of the amount of Lewis acid (Table 5, entries 1–3). At all three stoichiometries, a selectivity switch was observed in the presence of 2,6-DTBP. A much greater divergence of behavior was observed with tin(II) Lewis acids. Stannous fluoride induced cyclization afforded the *syn* aldol product with a ratio of 66:34 in the presence of 2,6-DTBP (Table 5, entry 4). Further investigation with SnCl$_2$ also showed *syn* selectivity with the ratio 79:21 (Table 5, entry 5). In both of cyclizations, there were no considerable differences in selectivity with or without 2,6-DTBP. Stannous bromide showed *anti* selectivity; however, it also showed *syn* selectivity in the

Table 5. Cyclization of **1** with Sn^{IV} and Sn^{II} salts.[a]

Entry	Lewis acid ([equiv])	*syn*-**2**/*anti*-**2**[b]	*syn*-**2**/*anti*-**2**[b,c]	$\Delta\Delta G^{\ne[c]}$ [kcal mol^{-1}]
1	SnCl$_4$ (0.5)	16:84	63:37	0.21
2	SnCl$_4$ (1.1)	18:82	61:39	0.17
3	SnCl$_4$ (2)	–	64:36	0.22
4	SnF$_2$ (1.1)	63:37	66:34	0.26
5	SnCl$_2$ (1.1)	78:22	79:21	0.51
6	SnBr$_2$ (1.1)	39:61	63:37	0.21
7	SnI$_2$ (1.1)	49:51	44:56	−0.09
8	Sn(OTf)$_2$ (1.1)	31:69	36:64	−0.22

[a] All cyclizations were performed in methylene chloride at −78 °C for 1 h. [b] Determined by capillary GC analysis, average of at least three runs within ±3%. [c] Reaction in the presence of 2,6-di-*tert*-butylpyridine.

presence of 2,6-DTBP (Table 5, entry 6). Stannous iodide showed slight *anti* selectivity under both conditions (Table 5, entry 7). In Table 5, entry 8, the highest *anti* selectivity was afforded by stannous triflate (*syn/anti* = 31:69).

A stoichiometry study with SnF_2 and $SnCl_2$ in cyclizations of model system **1** was performed, and the results are summarized in Table 6. In the first two experiments, 1.1 and

Table 6. Cyclization of **1** with tin(II) salts under various conditions.[a]

Entry	Lewis acid ([equiv])	Solvent	*syn-2/anti-2*[b]	*syn-2/anti-2*[b,c]	$\Delta\Delta G^{\neq}$[c] [kcal mol^{-1}]
1	SnF_2 (1.1)	CH_2Cl_2	63:37	66:34	0.26
2	SnF_2 (5)	CH_2Cl_2	66:34	67:33	0.27
3	SnF_2 (1.1)	THF	–	51:49	0.02
4	$SnCl_2$ (0.05)	CH_2Cl_2	incomplete	–	–
5	$SnCl_2$ (0.1)	CH_2Cl_2	incomplete	–	–
6	$SnCl_2$ (0.5)	CH_2Cl_2	74:26	–	0.41
7	$SnCl_2$ (1.1)	CH_2Cl_2	78:22	79:21	0.51
8	$SnCl_2$ (2)	CH_2Cl_2	84:16	–	0.64
9	$SnCl_2$ (5)	CH_2Cl_2	64:36	72:28	0.37

[a] All cyclizations were performed at −78 °C for 1 h. [b] Determined by capillary GC analysis, average of at least three runs within ±3 %. [c] Reaction in the presence of 2,6-di-*tert*-butylpyridine.

5 equivalents of SnF_2 were used, and they produced almost the same selectivity (Table 6, entries 1 and 2). When this reaction was performed in THF, the *syn* selectivity decreased to 51:49 (Table 6, entry 3) which suggests that SnF_2 acted primarily as a Lewis acid type catalyst. When 0.05 or 0.1 equivalents of $SnCl_2$ was used, the reaction did not go to completion (Table 6, entries 5 and 6). The use of 0.5, 1.1, and 2 equivalents of $SnCl_2$ resulted in *syn*-selective reactions (Table 6, entries 7–9). The highest *syn* selectivity was observed with 2 equivalents of $SnCl_2$, with a ratio of 84:16 (Table 6, entry 8). However, with 5 equivalents of $SnCl_2$, the *syn* selectivity decreased to 64:36. In the presence of 2,6-DTBP, a slight increase in *syn* selectivity was observed with a ratio of 72:28 (Table 6, entry 9).

To investigate the selectivity with other Lewis acids similar to tin(II), cyclizations of **1** with zinc(II) and magnesium(II) halides were carried out, and the results are summarized in Table 7. One equivalent of zinc(II) fluoride could not promote the reaction to completion, but 5 equivalents showed *anti* selectivity with a ratio of 35:65 (Table 7, entry 2). Apparently, zinc(II) fluoride acted as a fluoride source rather than a Lewis acid. The *anti* selectivity was reversed to *syn* in the cyclizations with $ZnCl_2$, $ZnBr_2$, and ZnI_2 (Table 7, entries 3–6), and no stereoselectivity was observed for $Zn(OTf)_2$ (Table 7, entry 7). Finally, magnesium bromide showed weak *anti* selectivity (Table 7, entry 8).

The results from fluoride ion induced cyclizations of **1** are summarized in Table 8. All reactions were performed in THF at −78 °C. The first four entries contain the results with different amounts of TBAF. When the loading of TBAF was changed from 0.05 to 10 equivalents, the reactions afforded almost the same *anti* selectivities (18:82–21:79; Table 8, entries 1–4). Cyclization at room temperature

Table 7. Cyclization of **1** with Zn^{II} and Mg^{II} salts.[a]

Entry	Lewis acid ([equiv])	*syn-2/anti-2*[b]	*syn-2/anti-2*[b,c]	$\Delta\Delta G^{\neq}$[c] [kcal mol^{-1}]
1	ZnF_2 (1.1)	incomplete	–	–
2	ZnF_2 (5)	37:63	35:65	−0.24
3	$ZnCl_2$ (1.1)	–	72:28	0.37
4	$ZnCl_2$ (5)	38:62	–	−0.19
5	$ZnBr_2$ (1.1)	40:60	71:29	0.35
6	ZnI_2 (1.1)	–	69:31	0.31
7	$Zn(OTf)_2$ (1.1)	–	53:47	0.05
8	$MgBr_2$ (1.1)	41:59	35:65	−0.24

[a] All cyclizations were performed in methylene chloride at −78 °C for 1 h. [b] Determined by capillary GC analysis, average of at least three runs within ±3 %. [c] Reaction in the presence of 2,6-di-*tert*-butylpyridine.

Table 8. Fluoride ion induced aldol reaction of **1**.[a]

Entry	Fluoride ion ([equiv])	T [°C]	t [h]	*syn-2/anti-2*[b]	$\Delta\Delta G^{\neq}$ [kcal mol^{-1}]
1	TBAF (0.05)	−78	24	19:81	−0.56
2	TBAF (0.1)	−78	24	19:81	−0.56
3	TBAF (1.1)	−78	24	18:82	−0.59
4	TBAF (10)	−78	24	21:79	−0.51
5	TBAF (0.1)	RT	2	22:78	−0.75
6	TBAF[c] (1.1)	−78	24	17:83	−0.61
7	TBAF/H_2O[d] (1.1)	−78	24	20:80	−0.54
8	TASF (0.05)	−78	1	incomplete	–
9	TASF (1.1)	−78	1	39:61	−0.17
10	TASF (5)	−78	1	40:60	−0.16
11	KF (1.1)	RT	12	incomplete	–
12	KF (10)	RT	12	incomplete	–
13	CsF (1.1)	RT	8	13:87	−1.13
14	KF/Kryptofix® [2.2.2] (1.1)	−78	24	9:91	−0.90

[a] All cyclizations were performed in THF. [b] Determined by capillary GC analysis. [c] TBAF solution was prepared from anhydrous solid TBAF. [d] A solution of TBAF containing 20 % water was used.

with 0.1 equivalents of TBAF also showed only slight changes (Table 8, entries 2 and 5). Because the commercially available solution of TBAF in THF contains about 5 % water, the effect of this contaminant was tested. To investigate the effect of water in the TBAF-induced cyclization of **1**, an "anhydrous" solution of TBAF and a solution of TBAF containing 20 % water were prepared. Following the methods of Cox et al. and Sharma and Fry,[30] TBAF·$3H_2O$ was dried under vacuum to afford "anhydrous" solid TBAF. However, there was no change in selectivity between the two different TBAF sources (Table 8, entries 6 and 7). All TBAF-induced cyclizations under different conditions gave almost the same selectivities.

Another reactive fluoride source, TASF, gave lower *anti* selectivity (Table 8, entries 9 and 10). The erosion of *anti* selectivity could be due to TMSF, which is produced from TASF.[20] Less-reactive fluoride sources (KF and CsF) were employed to examine the intervention of the "hexacoordinate silicon" T_{24} as proposed by Corriu and co-workers.[21] In the presence of KF, the reaction did not go to completion because KF is only sparingly soluble in THF (Table 8, entries 11 and 12). Cesium fluoride induced cyclization showed

high *anti* selectivity, which implies that the cyclization proceeded via the naked enolate (Table 8, entry 13). Solubilization of KF with Kryptofix 222 led to the highest *anti* selectivity with the ratio 9:91 (Table 8, entry 14). This result is in agreement with that of the cyclization of the same model system with KHMDS in the presence of Kryptofix 222.[25]

Discussion

Lewis Acids

For the rationalization of the overall *anti* selectivity observed in Lewis acid induced cyclizations of **1** (except with tin Lewis acids), two transition-state structures T_{22} and T_{23} are proposed (Scheme 20). In both of structures, the Lewis acid occupies a coordination site on the aldehyde oxygen atom *cis* to the aldehyde hydrogen atom. The synclinal T_{22} should have two destabilizing factors. First, there is an unfavorable dipole–dipole interaction between the two carbon–oxygen bonds in the synclinal disposition. This effect mirrors the rationalization of *anti* selectivity of Heathcock et al. through open transition-state structures.[12b] Another

Scheme 20. Proposals of transition-state structures for the Lewis acid induced cyclizations of **1**.

destabilizing factor in T_{22} might be the nonbonding steric interactions between the silyloxy group and the Lewis acid–aldehyde complex. Empirically, the similar selectivities for Lewis acids of different sizes (Tables 1–4) implies that this factor is not important. Therefore, the antiperiplanar transition-state structure T_{23} should be favored because of the unfavorable dipole–dipole interaction between the two carbon–oxygen bonds in the synclinal disposition of T_{22}. The insensitivity of the cyclization to the size and nature of the Lewis acid emphasizes the absence of an intrinsic steric bias. Moreover, the modest selectivity reveals a weak intrinsic preference for a double-bond orientation consistent with the well-documented variation in selectivity with enol geometry, substitution, and aldehyde structure.

The stereoselectivity observed for tin(II) Lewis acids in Tables 5–7 can be rationalized by transition-state structures T_{26} and T_{27} (Scheme 20). There must be a significant difference between tin Lewis acids and most of the Lewis acids that gave an overall *anti* preference. Apparently, the tin Lewis acids are able to coordinate both the enol and aldehyde oxygen atoms. In the case of tin(IV) Lewis acids, therefore, the "bridging halometallate" transition-state structure T_{26}, which affords the *syn* aldol adduct, must be weakly favored over the antiperiplanar T_{23}. The selectivity of tin(II) Lewis acid induced cyclizations depends on the counterion of the tin(II) salt. In the synclinal transition-state structure T_{27}, the halide bound to the metal is close to the silicon moiety, so it can function in the cyclization as a coordinating and desilylating agent.

Similar cyclic transition-state structures in the Lewis acid induced Mukaiyama aldol reaction between a silyl enol ether or a ketene silyl acetal and an aldehyde were proposed by Chan et al.,[31] Barner et al.,[17] Helmchen et al.,[32] and Yamamoto and co-workers.[18] In these proposals, the metal is coordinated to both the aldehyde and enolate oxygen atoms, and a halide ion then attacks the silicon atom to create a bicyclic transition-state structure. In view of the affinity of titanium, silver, and other metals for oxygen, the chairlike transition-state structure might explain the high stereoselectivity.

In the cyclic transition-state structure T_{27}, Sn^{II} is proposed to be strongly coordinated to the two oxygen atoms. Although many tin(II) compounds behave as monodentate acceptors towards donor molecules, some complexes that contain additional ligands are known.[33] The distorted, trigonal-bipyramidal coordination geometry depicted in T_{27} is supported by the X-ray structures of $SnX_2(1,4\text{-dioxane})$.[34] In the X-ray study of $SnCl_2(1,4\text{-dioxane})$, the tin(II) atom is described as a distorted trigonal bipyramid with the fifth ligand position occupied by a stereochemically active lone electron pair. The repulsion between the Sn—O bonding electrons and lone-pair electrons may be relieved either by a reduction in the O—Sn—O angle or by a lengthening of the Sn—O bonds. Actually, the Sn—O bond length in $SnCl_2(1,4\text{-dioxane})$ is 0.2–0.39 Å longer than that in tin(II) chloride dihydrate[35a] and bis(1-phenylbutane-1,3-dionato)tin(II).[35b] In
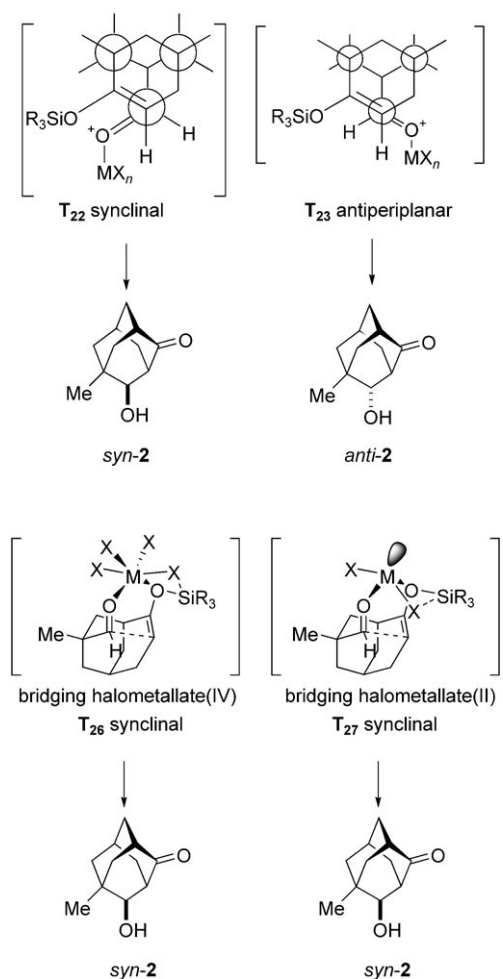
SnBr$_2$(1,4-dioxane), there is a larger decrease in the O–Sn–O angle compared to the isostructural chloride.

The selectivity induced by tin(II) salts was strongly influenced by the nature of the counterion, except in the case of stannous fluoride. Because stannous fluoride can behave both as a Lewis acid and a fluoride source, the result cannot be interpreted solely in terms of a single mode of activation. The magnitude of the *syn* preference decreased in the order Cl > Br > I > OTf. In **T$_{27}$**, the tin atom exists as a distorted trigonal bipyramid with a stereochemically active lone electron pair (Scheme 21). The tin atom is strongly coordinated to the two oxygen atoms and the X groups, which explains why the selectivity is counterion-dependent.
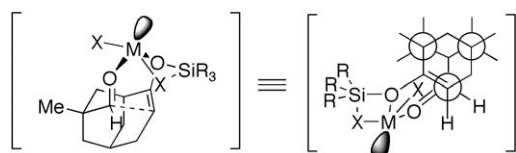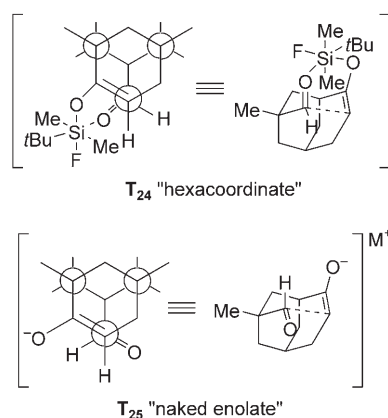

Scheme 21. Synclinal transition-state structure **T$_{27}$** of a bridging halo-metallate.

Fluoride Ion

In the case of fluoride-induced cyclizations of model system **1**, two possible transition-state structures **T$_{24}$** and **T$_{25}$** are proposed (Scheme 22). Transition-state structure **T$_{24}$** invokes a "hypervalent silicon" intermediate. Upon coordination of a fluoride anion, the resulting "pentacoordinate siliconate" has enhanced Lewis acidity[23] and could coordinate to the aldehyde oxygen atom to produce the "hexacoordinate siliconate" **T$_{24}$**. In this transition-state structure, the "hexacoordinate" silicon should produce aldol product *syn-***2**. Corriu and co-workers proposed this intermediate for reactions induced by less-reactive fluorides such as CsF and KF.[21]

Another transition-state structure for the fluoride ion induced cyclization of **1** is the "naked enolate" **T$_{25}$**. This structure has been invoked for very reactive fluoride sources such as TASF and *n*Bu$_4$N$^+$F$^-$. In this case, the same intermediate "pentacoordinate siliconate" is attacked by another fluoride ion rather than an aldehyde oxygen atom. By losing TMSF$_2$, the "naked enolate" is produced. This pathway was suggested by Noyori, Kuwajima, and co-workers.[20] It is known that the "naked enolate" **T$_{25}$** produces aldol product *anti-***2** from the antiperiplanar disposition of the two carbon–oxygen bonds to minimize dipole–dipole interactions.[25]

The TBAF-induced cyclization of model system **1** showed *anti* selectivity, which implies that the cyclization of **1** proceeds through the naked enolate transition-state structure **T$_{25}$**. The antiperiplanar disposition of the enolate and aldehyde oxygen atoms minimizes the Coulombic dipole repulsions, thus affording the *anti* product. The hexacoordinate structure **T$_{24}$** is not energetically favorable under these conditions.

Conclusions

Model compound **1** was designed and successfully synthesized to examine the relative orientation of silyl enol ethers and carbonyl moieties in the transition-state structures of the Mukaiyama directed aldol reaction. This study revealed a modest, intrinsic preference for antiperiplanar geometry (open transition-state structure). The *anti* preference was for the most part independent of the nature and stoichiometry of the Lewis acid. For both SnCl$_4$ and SnCl$_2$, *syn* selectivity was observed, but the selectivity was stronger for SnCl$_2$ and was counterion-dependent. All fluoride-induced cyclizations proceeded with antiperiplanar geometry, most likely via a naked enolate that experiences strong dipole repulsions. No evidence for a hypercoordinate siliconate was obtained.

Experimental Section

General

Solvents for chromatography and extraction were of technical grade and were distilled from the drying agents indicated: hexane (CaH$_2$ or K$_2$CO$_3$), dichloromethane (CaH$_2$), diethyl ether and *tert*-butyl methyl ether (CaSO$_4$/FeSO$_4$), ethyl acetate (K$_2$CO$_3$). Column chromatography was performed with 32–63-mm silica gel (Merck) and basic or neutral alumina. All reactions were performed in oven- or flame-dried glassware under an inert atmosphere of dry N$_2$. All solvents used in the reactions were distilled from appropriate drying agents before use. Melting points were determined on a Thomas–Hoover capillary melting-point apparatus and are uncorrected. Analytical TLC was performed on Merck silica-gel plates with QF-254 indicator. Infrared (IR) spectra were obtained on an IBM FTIR-32 spectrophotometer. Peaks are reported in cm^{-1} with the following relative intensities: br (broad), s (strong, 67–100%), m (medium, 34–66%), w (weak, 0–33%). ^{1}H and ^{13}C NMR spectra were recorded on a General Electric QE-300 (300 MHz for ^{1}H, 75.5 MHz for ^{13}C) or Varian U-400 (400 MHz for ^{1}H, 100.6 MHz for ^{13}C) spectrometer. Chemical shifts (δ) are reported in ppm, and coupling constants (*J*) are reported in Hz. Multiplicities are indicated by s (singlet), d (doublet), t (triplet), q (quartet), m (multiplet), and br (broad). Assignments of individual resonances were supported by APT (attached proton test), DEPT (distortionless enhancement by polarization transfer), HETCOR (hetero-correlation), and/or COSY. Mass spectra were recorded on a Varian MAT CH-5 spectrometer with ionization voltages of 70 eV, or on a VSE-

Scheme 22. Transition-state structures for the fluoride-promoted cyclization of **1**.

70 spectrometer with isobutane gas as the CI (chemical ionization) reagent gas. Analytical gas chromatography was performed on a Varian 3700 or Hewlett–Packard 5890 chromatograph equipped with split and on-column injectors and a flame ionization detector. The carrier gas was H_2 (1 mL min^{-1}) for capillary columns. The columns used were an HP-1 (50 m) or a Carbowax 20M (50 m). The injector temperature was 225 °C, the detector temperature was 300 °C, flow rates were approximately 30 mL min^{-1} for H_2 and N_2 and 100 mL min^{-1} for air, and programs were as indicated. Programs are reported in the form: initial temperature (time), temperature ramp rate, final temperature (time). Retention times (t_R) and integrated ratios were obtained from a Hewlett Packard 3390A or 3393A integrator. *n*-Butyllithium was titrated according to the method of Gilman and Schulze.[36] Borane/THF and DIBALH were standardized by the analytical gas titration method of Brown and Ravindran.[37]

Syntheses

5: A flame-dried, 250-mL flask equipped with a magnetic stirrer bar and a nitrogen inlet was charged with a solution of **3** (3.19 g, 11.13 mmol) in methylene chloride (100 mL) at room temperature. Trimethylsilyl 2-methyl-2-trimethylsiloxypropanoate (**4**; 3.32 g, 13.35 mmol) and a catalytic amount of 2,6-DTBP (50 μL, 0.22 mmol) were added. The resulting solution was stirred for 5 min at room temperature, and a catalytic amount of trimethylsilyltrifluoromethanesulfonate (86 μL, 0.45 mmol) was added dropwise. The resulting clear solution was stirred for 36 h at room temperature, after which it dark yellow. The reaction mixture was poured into water (50 mL) and extracted with *tert*-butyl methyl ether (3× 200 mL). The organic extracts were combined, dried over Na_2SO_4, and concentrated. Purification of the residue by column chromatography (ethyl acetate/hexane = 1:20, 1:20, 1:10, 1:10, 1:5, 1:5) afforded (*R,S*)-(1*l*,2*u*,5*u*,7*u*,2″*x*)-2-benzoyloxy-7-[2-(5,5-dimethyl-1,3-dioxolan-4-onyl)]-7-methylbicyclo[3.3.1]nonane (**5**; 3.86 g, 93%) as a white solid. An analytical sample was obtained by recrystallization from hexane. R_f = 0.52 (hexane/EtOAc = 4:1); m.p.: 113–114 °C (hexane); IR (CCl$_4$): $\tilde{v}$ = 2938 (m), 1806 (s), 1717 (s), 1453 (w), 1383 (w), 1269 (s), 1180 (m), 1107 (m), 1071 (m), 988 cm^{-1} (w); ^{1}H NMR (300 MHz, CDCl$_3$): δ = 8.08–8.05 (m, 2H, HC3′, HC7′), 7.59–7.53 (m, 1H, HC5′), 7.47–7.42 (m, 2H, HC4′, HC6′), 5.18 (s, 1H, HC2″O$_2$), 4.94 (br s, 1H, HC2O), 2.30 (d, *J* = 11.2 Hz, 1H, HC1), 2.20–2.16 (m, 1H, HC5), 2.13–2.04 (m, 1H, HC3), 1.92–1.77 (m, 3H, H$_2$C6, HC3), 1.75–1.66 (m, 3H, HC8, HC9, HC4), 1.51 (s, 3H, H$_3$C6″), 1.44 (s, 3H, H$_3$C6″), 1.48–1.36 (m, 3H, HC8, HC9, HC4), 1.21 ppm (s, 3H, H$_3$C10); ^{13}C NMR (75.5 MHz, CDCl$_3$): δ = 175.8 (C= O4″), 165.7 (C=O1′), 132.7 (C5′), 131.0 (C2′), 129.5 (C3′, C7′), 128.3 (C4′, C6′), 108.0 (HC2″O$_2$), 77.3 (H$_3$C6), 77.3 (H$_3$C6), 75.1 (OC2H), 34.2 (C7), 31.7 (H$_2$C8), 31.4 (H$_2$C8), 30.2 (H$_2$C6), 30.1 (H$_2$C9), 30.0 (H$_2$C6), 28.3 (HC1), 28.2 (HC1), 27.7 (H$_3$C10), 27.5 (H$_3$C10), 24.1 (H$_3$C6″), 23.3 (HC5), 23.2 (HC5), 22.5 (H$_2$C3), 21.6 (H$_3$C6″), 20.6 (H$_2$C4), 20.6 ppm (H$_2$C4); MS (CI, *iso*-butane): *m/z* (%) = 372 [*M*]$^+$ (0.2), 251 (17), 166 (17), 165 (100), 147 (13), 105 (11); elemental analysis: calcd (%) for C$_{22}$H$_{28}$O$_5$ (372.47): C 70.94, H 7.58; found: C 71.11, H 7.63.

6: A flame-dried, 250-mL flask equipped with a magnetic stirrer bar and a nitrogen inlet was charged with a solution of **5** (3.20 g, 8.59 mmol) in methylene chloride (100 mL). After the mixture was cooled to −78 °C, a solution of DIBALH in hexane (1 M, 19 mL, 18.90 mmol) was added dropwise over 5 min. The resulting solution was stirred for 1 h at −78 °C, and water (30 mL) was added dropwise. The cold bath was removed, the reaction mixture was allowed to warm to room temperature, and the reaction mixture was poured into water (200 mL) and extracted with *tert*-butyl methyl ether (3×200 mL). The organic extracts were combined, dried over Na_2SO_4, and concentrated. Purification of the residue by column chromatography (hexane/ethyl acetate = 10:1, 5:1, 2:1, 1:1) afforded (*R,S*)-(1*l*,2*u*,5*u*,7*u*,2′*x*,4′*x*)-7-[2-(5,5-dimethyl-4-hydroxy-1,3-dioxolanyl)]-2-hydroxy-7-methylbicyclo[3.3.1]nonane (**6**; 2.18 g, 94%) as a white solid. An analytical sample was obtained by recrystallization from hexane. R_f = 0.05 (hexane/EtOAc = 4:1); m.p.: 118–119 °C (hexane); IR (CCl$_4$): $\tilde{v}$ = 3393 (m), 3289 (m), 2977 (m), 2934 (s), 1551 (w), 1453 (w), 1364 (m), 1254 (w), 1175 (w), 1090 (s), 1001 (s), 963 cm^{-1} (s); ^{1}H NMR (300 MHz, CDCl$_3$): δ = 5.10 (d, *J* = 4.2 Hz, 0.8 H, HO*H*C4′O), 5.00 (d, *J* = 8.0 Hz, 0.2 H, HO*H*C4′O), 4.87 (s, 0.8 H, HC2′O$_2$), 4.68 (s, 0.2 H,

HC2′O$_2$), 3.66 (br s, 1H, *H*C2OH), 2.83 (d, *J* = 4.4 Hz, 0.8 H, *H*OHC4′O), 2.35 (d, *J* = 8.1 Hz, 0.2 H, *H*OHC4′O), 2.06–1.96 (m, 3H, HC1, HC5, HC3), 1.82–1.71 (m, 3H, H$_2$C6, HC3), 1.65–1.55 (m, 3H, HC8, HC9, HC4), 1.44–1.40 (m, 2H, HC8, HC9), 1.29 (s, 4.8 H, H$_3$C6′), 1.24 (s, 1.2 H, H$_3$C6′), 1.21 (br m, 1H, HC4), 1.15 (s, 0.6 H, H$_3$C10), 1.12 ppm (s, 2.4 H, H$_3$C10); ^{13}C NMR (75.5 MHz, CDCl$_3$): δ = 109.5 (HC2′O$_2$), 109.5 (HC2′O$_2$), 108.6 (HC2′O$_2$), 108.6 (HC2′O$_2$), 100.5 (HOHC4′O), 99.0 (HOHC4′O), 81.6 ((CH$_3$)$_2$CO5′), 72.6 (HC2OH), 72.6 (HC2OH), 72.5 (HC2OH), 33.7 (C7), 33.7 (C7), 32.8 (H$_2$C8), 32.6 (H$_2$C8), 32.4 (H$_2$C8), 31.8 (H$_2$C9), 31.5 (H$_2$C9), 31.4 (H$_2$C9), 31.3 (HC1), 29.3 (HC6), 27.4 (H$_3$C10), 27.2 (H$_3$C10), 26.3 (HC5), 23.7 (H$_3$C6′), 23.6 (H$_3$C6′), 23.0 (H$_2$C3), 23.0 (H$_2$C3), 22.2 (H$_3$C6′), 22.2 (H$_3$C6′), 21.5 (H$_2$C4), 20.2 ppm (H$_3$C6′); MS (CI, *iso*-butane): *m/z* (%) = 269 [*M*−1]$^+$ (2), 253 (47), 166 (15), 165 (100), 147 (39); elemental analysis: calcd (%) for C$_{15}$H$_{26}$O$_4$ (270.37): C 66.64, H 9.69; found: C 66.62, H 9.71.

7: A flame-dried, 500-mL flask equipped with a magnetic stirrer bar and a nitrogen inlet was charged with a solution of the oxalyl chloride (1.4 mL, 15.95 mmol) in methylene chloride (100 mL). After the mixture was cooled to −78 °C, a solution of DMSO (2.26 mL, 31.90 mmol) in methylene chloride (30 mL) was added dropwise. After 10 min, a solution of **6** (1.96 g, 7.25 mmol) in methylene chloride (100 mL) was added dropwise at −78 °C. The resulting clear solution turned into a white turbid suspension after 5 min at −78 °C. After 40 min, triethylamine (8.08 mL, 57.99 mmol) was added dropwise, the cold bath was removed, and the reaction mixture was allowed to warm to room temperature. The reaction mixture was poured into water (200 mL) and extracted with *tert*-butyl methyl ether (3×200 mL). The organic extracts were combined, dried over Na_2SO_4, and concentrated. Purification of the residue by column chromatography (hexane/ethyl acetate = 20:1, 10:1, 5:1, 2:1) afforded (*R,S*)-(1*l*,5*u*,7*u*,2′*x*)-7-[2-(5,5-dimethyl-1,3-dioxolan-4-onyl)]-7-methylbicyclo[3.3.1]nonan-2-one (**7**; 1.70 g, 88%) as a white solid. An analytical sample was obtained by recrystallization from hexane. R_f = 0.25 (hexane/ EtOAc = 4:1); m.p.: 71–72 °C (hexane); IR (CCl$_4$): $\tilde{v}$ = 2936 (m), 1804 (s), 1713 (s), 1468 (w), 1383 (m), 1344 (w), 1279 (m), 1208 (s), 1183 (m), 1157(m), 1078 (m), 978 (m); ^{1}H NMR (300 MHz, CDCl$_3$): δ = 5.20 (s, 0.25 H, HC2′O$_2$), 5.19 (s, 0.75 H, HC2′O$_2$), 2.55–2.40 (m, 3H, HC1, H$_2$C3), 2.33–2.01 (m, 3H, H$_2$C6, HC5), 1.90–1.76 (m, 3H, HC8, HC9, HC4), 1.73–1.47 (m, 3H, HC8, HC9, HC4), 1.46 (s, 0.75 H, H$_3$C6′), 1.24 (s, 2.25 H, H$_3$C6′), 1.38 (s, 3H, H$_3$C6′), 1.03 (s, 0.75 H, H$_3$C10), 1.01 ppm (s, 2.25 H, H$_3$C10); ^{13}C NMR (75.5 MHz, CDCl$_3$): δ = 216.5 (O=C2), 216.4 (O=C2), 175.6 (O=C4′O), 175.1 (O=C4′O), 104.7 (HC2′O$_2$), 104.4 (HC2′O$_2$), 77.3 ((CH$_3$)$_2$C5′O), 77.2 ((CH$_3$)$_2$C5′O), 41.9 (HC1), 41.9 (HC1), 37.3 (H$_2$C3), 36.4 (H$_2$C3), 35.8 (C7), 35.6 (C7), 35.4 (H$_2$C8), 35.3 (H$_2$C8), 34.3 (H$_2$C6), 34.1 (H$_2$C6), 28.3 (H$_2$C9), 28.2 (H$_2$C9), 27.9 (H$_2$C4), 27.9 (H$_2$C4), 24.9 (H$_3$C10), 24.5 (H$_3$C10), 23.9 (HC5), 23.7 (H$_3$C6′), 23.8 (H$_3$C6′), 21.2 (H$_3$C6′), 20.0 ppm (H$_3$C6′); MS (CI, *iso*-butane): *m/z* (%) = 267 [*M*+1]$^+$ (100), 181 (36), 165 (10), 163 (76), 69 (13); elemental analysis: calcd (%) for C$_{15}$H$_{22}$O$_4$ (266.34): C 67.65, H 8.33; found: C 67.68, H 8.35.

8: A flame-dried, 50-mL flask equipped with a magnetic stirrer bar and a nitrogen inlet was charged with a solution of **7** (131.0 mg, 0.49 mmol) in THF (15 mL). After the mixture was cooled to −95 °C with an acetone/ liquid-nitrogen bath, TBSOTf (0.16 mL, 0.69 mmol) was added neat at −95 °C. After 3 min, a solution of KHMDS in THF (0.61 M, 0.97 mL, 0.59 mmol) was added dropwise. After 5 min, pH 9 buffer (10 mL) was added dropwise, the cold bath was removed, and the reaction mixture was allowed to warm to room temperature. The reaction mixture was extracted with hexane (3×200 mL), and the organic extracts were combined, dried over Na_2SO_4, and concentrated. Purification of the residue by cold column chromatography on Activity III neutral alumina (hexane for 20 fractions, then hexane/ethyl acetate = 20:1, 10:1) with a jacketed column with circulating cold (−78 °C) acetone afforded (*R,S*)-(1*l*,5*u*,7*u*,2′*x*)-2-*tert*-butyldimethylsiloxy-7-[2-(5,5-dimethyl-1,3-dioxolan-4-onyl)]-7-methylbicyclo[3.3.1]non-2-ene (**8**; 169 mg, 90%) as a clear, colorless oil. R_f = 0.85 (hexane/EtOAc = 4:1); IR (CCl$_4$): $\tilde{v}$ = 2930 (s), 2859 (m), 1800 (s), 1665 (w), 1549 (w), 1462 (w), 1381 (w), 1254 (m), 1204 (s), 1184 (m), 1152 (m), 986 (w), 963 (w), 841 cm^{-1} (s); ^{1}H NMR (300 MHz, CDCl$_3$): δ = 6.07 (s, 0.55 H, HC2′O$_2$), 6.03 (s, 0.45 H, HC2′O$_2$), 4.63 (dd, *J* = 7.4, 4.0 Hz, 1H, HC3), 2.43 (dd, *J* = 6.7, 2.1 Hz, 0.45 H, HC4), 2.37

(dd, $J = 6.9$, 2.3 Hz, 0.55 H, HC4), 2.23 (s, 0.45 H, HC8), 2.18–2.15 (m, 0.55 H, HC8), 2.11 (s, 1 H, HC1), 2.11–1.99 (m, 1 H, HC5), 1.99 (s, 0.45 H, HC6), 1.94–1.93 (m, 0.55 H, HC6), 1.90 (t, $J = 4.5$ Hz, 0.55 H, HC4), 1.85 (dd, $J = 9.2$, 4.2 Hz, 0.45 H, HC4), 1.68–1.66 (m, 0.45 H, HC9), 1.64 (d, $J = 0.9$ Hz, 0.55 H, HC9), 1.56 (d, $J = 4.9$ Hz, 1 H, HC9), 1.53–1.48 (m, 1 H, HC6), 1.43 (s, 3 H, H_3C6'), 1.34 (d, $J = 1.1$ Hz, 3 H, H_3C6'), 1.31–1.22 (m, 1 H, HC8), 0.92 (d, $J = 2.1$ Hz, 9 H, $(H_3C)_3CSi$), 0.88 (s, 3 H, H_3C10), 0.13 (d, $J = 7.3$ Hz, 3 H, $(H_3C)Si$), 0.13 ppm (s, 3 H, $(H_3C)Si$); ^{13}C NMR (75.5 MHz, $CDCl_3$): $\delta = 176.3$ (O=C4'O), 176.0 (O=C4'O), 155.3 (CH=$C2$), 155.2 (CH=$C2$), 104.5 (HC2'O_2), 104.2 (HC2'O_2), 101.8 (C=$C3H$), 100.9 (C=$C3H$), 77.3 (($CH_3)_2C5'O$), 77.2 (($CH_3)_2C5'O$), 40.0 (C7), 39.2 (C7), 36.2 (H_2C8), 36.1 (H_2C8), 34.5 (H_2C6), 34.1 (C1), 33.9 (H_2C6), 31.5 (H_2C9), 31.4 (H_2C9), 30.9 (H_2C4), 30.6 (H_2C4), 25.7 (H_3C10), 25.7 (H_3C10), 25.6 (Si$C(CH_3)_3$), 25.6 (Si$C(CH_3)_3$), 24.5 (H_3C6'), 24.3 (H_3C6'), 24.2 (H_3C6'), 24.0 (H_3C6'), 21.7 (HC5), 21.4 (HC5), 17.9 (Si$C(CH_3)_3$), 17.9 (Si$C(CH_3)_3$), −4.26 (SiCH_3), −4.37 (SiCH_3), −4.55 (SiCH_3), −4.94 ppm (SiCH_3); MS (CI, *iso*-butane): m/z (%) = 381 $[M]^+$ (100), 237 (24), 163 (31), 133 (22), 75 (10); elemental analysis: calcd (%) for $C_{21}H_{36}O_4Si$ (380.60): C 66.27, H 9.53; found: C 66.10, H 9.56.

1: A flame-dried, 50-mL flask equipped with a magnetic stirrer bar and a nitrogen inlet was charged with a solution of **8** (116 mg, 0.31 mmol) in THF (15 mL). After the mixture was cooled to 0 °C, a 5 % solution of NaOH in methanol (0.16 mL, 0.69 mmol) was added dropwise. After 5 min, pH 9 buffer (10 mL) was added dropwise, the cold bath was removed, and the reaction mixture was allowed to warm to room temperature. The reaction mixture was extracted with hexane (3 × 200 mL), and the organic extracts were combined, dried over Na_2SO_4, and concentrated. Purification of the residue by cold column chromatography on Activity V basic alumina (hexane only) with a jacketed column with circulating cold (−78 °C) acetone afforded (R,S)-(1l,5u,7u)-2-*tert*-butyldimethylsiloxy-7-formyl-7-methylbicyclo[3.3.1]non-2-ene (**1**; 78 mg, 87 %) as a clear, colorless oil, which solidified in the freezer. IR (neat): $\tilde{v} = 3453$ (w), 2928 (s), 2857 (s), 2705 (w), 1719 (m), 1663 (m), 1462 (m), 1379 (w), 1296 (w), 1254 (m), 1198 (m), 1098 (m), 1044 (m), 1005 (w), 936 (w), 916 cm^{-1} (w); ^1H NMR (400 MHz, C_6D_6): $\delta = 9.42$ (d, $J = 1.6$ Hz, 1 H, OHC10), 4.61 (dd, $J = 4.7$, 2.6 Hz, 1 H, HC3), 2.34 (dd, $J = 13.7$, 2.1 Hz, 1 H, HC8), 2.25 (dd, $J = 13.5$, 2.2 Hz, 1 H, HC6), 2.14 (dd, $J = 17.0$, 6.7 Hz, 1 H, HC4), 2.07–2.06 (m, 1 H, HC1), 1.97 (dd, $J = 17.4$, 4.6 Hz, 1 H, HC4), 1.72–1.70 (m, 1 H, HC5), 1.54–1.51 (m, 1 H, HC9), 1.23–1.21 (m, 1 H, HC9), 1.10 (dd, $J = 13.7$, 3.7 Hz, 1 H, HC6), 1.01–1.00 (m, 1 H, HC8), 0.97 (s, 9 H, $(H_3C)_3CSi$), 0.60 (s, 3 H, H_3C11), 0.15 (s, 3 H, $(H_3C)Si$), 0.08 ppm (s, 3 H, $(H_3C)Si$); ^{13}C NMR (100.6 MHz, C_6D_6): $\delta = 202.7$ (CHO10), 152.0 (CH=$C2$), 104.0 (C=$C3H$), 44.2 (C7), 38.0 (H_2C8), 36.9 (H_2C6), 34.8 (HC1), 31.9 (H_2C9), 29.6 (H_2C4), 26.5 (H_3C11), 26.4 (HC5), 25.8 (Si$C(CH_3)_3$), 18.1 (Si$C(CH_3)_3$), −4.37 (SiCH_3), −4.60 ppm (SiCH_3); MS (CI, *iso*-butane): m/z (%) = 296 $[M+1]^+$ (27), 295 $[M]^+$ (100), 237 (33), 181 (48), 164 (17), 163 (99), 133 (11): elemental analysis: calcd (%) for $C_{17}H_{30}O_2Si$ (294.51): C 69.33, H 10.27; found: C 69.16, H 10.32.

*General Procedure for Cyclization of Model System **1** with Representative Lewis Acids or Fluorides*

A magnetically stirred solution of **1** (≈ 0.01 M) in dry CH_2Cl_2 (or THF for fluoride-induced reactions) was cooled to −78 °C. The appropriate Lewis acid or fluoride ion (1.1 equiv) was added neat or as a stock solution in CH_2Cl_2, and the reaction mixture was stirred at −78 °C for 1 h. The reaction was quenched at −78 °C by addition of pH 9 buffer (0.1 mL), the cold bath was removed, and the reaction mixture was allowed to warm to room temperature. Water (2 mL) was added, and the mixture was extracted with *tert*-butyl methyl ether (2 × 2 mL). The organic layers were combined, dried over Na_2SO_4, and concentrated. The residue was dissolved in THF (0.1 M), and TBAF (10 equiv) was added at room temperature. The mixture was stirred for 3 h, and pH 9 buffer (0.1 mL) was added. The mixture was extracted with *tert*-butyl methyl ether (2 × 2 mL). The organic layers were combined and dried over Na_2SO_4. Analysis of the product ratios was accomplished by injection into a Hewlett–Packard 50-m Carbowax 20M capillary column. Final ratios were calculated on the basis of independently obtained response factors relative to the cyclododecane internal standard: GC Program: 100 (5 min), 20 °C min^{-1}, 165 (50 min). *syn*-**2**: $t_R = 50.69$ min; *anti*-**2**: $t_R = 48.03$ min.[29]

Acknowledgements

[1] T. Mukaiyama, *Challenges in Synthetic Organic Chemistry*, Oxford University Press, New York, **1994**.

[2] a) T. Mukaiyama, K. Narasaka, K. Banno, *Chem. Lett.* **1973**, *2*, 1011–1014; b) K. Saigo, M. Osaki, T. Mukaiyama, *Chem. Lett.* **1975**, *4*, 989–990.

[3] A. Nielsen, W. Houlihan, *Org. React.* **1968**, *16*, 1–438.

[4] a) T. Mukaiyama, *Org. React.* **1982**, *28*, 203–331; b) T. Mukaiyama, S. Kobayashi, *Org. React.* **1994**, *46*, 1–103.

[5] a) E. M. Carreira in *Comprehensive Asymmetric Catalysis, Vol. III* (Eds.: E. N. Jacobsen, A. Pflatz, H. Yamamoto), Springer-Verlag, Heidelberg, **1999**, chap. 29; b) M. Swamura, Y. Ito in *Catalytic Asymmetric Synthesis, 2nd ed.* (Ed.: I. Ojima), Wiley-VCH, Weinheim, **2000**, chap. 8B1; c) E. M. Carreira, A. Fettes, C. Marti, *Org. React.* **2006**, *67*, 1–216.

[6] a) C. Gennari in *Comprehensive Organic Synthesis, Vol. 2, Additions to C−X π Bonds, Part 2* (Ed.: C. H. Heathcock), Pergamon Press, Oxford, **1991**, pp. 629–660; b) E. M. Carreira in *Modern Carbonyl Chemistry* (Ed.: J. Otera), Wiley-VCH, Weinheim, **2000**, chap. 8; c) T. Mukaiyama, J. Matsuo in *Modern Aldol Reactions, Vol. 1* (Ed.: R. Mahrwald), Wiley-VCH, Weinheim, **2004**, chap. 3.

[7] For excellent, comprehensive reviews, see reference [5].

[8] T. Mukaiyama, K. Banno, K. Narasaka, *J. Am. Chem. Soc.* **1974**, *96*, 7503–7509.

[9] a) T. Chan, M. Brook, *Tetrahedron Lett.* **1985**, *26*, 2943–2946; b) G. Morris, R. Freeman, *J. Am. Chem. Soc.* **1979**, *101*, 760–762; c) R. Helmer, R. West, *Organometallics* **1982**, *1*, 877–879.

[10] I. Kuwajima, E. Nakamura, *Acc. Chem. Res.* **1985**, *18*, 181–187.

[11] a) S. Shambayati, W. Crowe, S. L. Schreiber, *Angew. Chem.* **1990**, *102*, 273–290; *Angew. Chem. Int. Ed. Engl.* **1990**, *29*, 256–272; b) S. Shambayati, S. Schreiber in *Comprehensive Organic Synthesis, Vol. 1, Additions to C−X π Bonds, Part 1* (Ed.: S. Schreiber), Pergamon Press, Oxford, **1991**, pp. 283–324; c) *Lewis Acids in Organic Synthesis* (Ed.: H. Yamamoto), Wiley-VCH, Weinheim, **2000**.

[12] a) C. H. Heathcock, K. Hug, L. A. Flippin, *Tetrahedron Lett.* **1984**, *25*, 5973–5976; b) C. H. Heathcock, S. Davidsen, K. Hug, L. A. Flippin, *J. Org. Chem.* **1986**, *51*, 3027–3037; c) C. H. Heathcock, L. Flippin, *J. Am. Chem. Soc.* **1983**, *105*, 1667–1668.

[13] C. H. Heathcock, C. Buse, W. Kleschick, M. Pirrung, J. Sohn, J. Lampe, *J. Org. Chem.* **1980**, *45*, 1066–1081.

[14] a) C. Gennari, M. Beretta, A. Bernardi, G. Moro, C. Scolastico, R. Todeschini, *Tetrahedron* **1986**, *42*, 893–909; b) C. Gennari, A. Bernardi, S. Cardani, C. Scolastico, *Tetrahedron Lett.* **1985**, *26*, 797–800.

[15] C. S. Wilcox, R. Babston, *J. Org. Chem.* **1984**, *49*, 1451–1453.

[16] T. Mukaiyama, S. Kobayashi, M. Murakami, *Chem. Lett.* **1985**, *14*, 447–450.

[17] B. Barner, Y. Liu, A. Rahman, *Tetrahedron* **1989**, *45*, 6101–6112.

[18] a) A. Yanigasawa, Y. Matsumoto, H. Nakashima, K. Asakawa, H. Yamamoto, *J. Am. Chem. Soc.* **1997**, *119*, 9319–9320; b) A. Yanigasawa, Y. Matsumoto, H. Nakashima, K. Asakawa, H. Yamamoto, *J. Am. Chem. Soc.* **1999**, *121*, 892–893; c) A. Yanigasawa, Y. Matsumoto, H. Nakashima, K. Asakawa, H. Yamamoto, *Tetrahedron* **2002**, *58*, 8331–8339.

[19] a) E. Nakamura, M. Shimizu, I. Kuwajima, *Tetrahedron Lett.* **1976**, *17*, 1699–1702; b) E. Nakamura, S. Yamago, D. Machii, I. Kuwajima, *Tetrahedron Lett.* **1988**, *29*, 2207–2210.

[20] a) R. Noyori, K. Yokoyama, J. Sakata, I. Kuwajima, E. Nakamura, M. Shimizu, *J. Am. Chem. Soc.* **1977**, *99*, 1265–1267; b) R. Noyori, I. Nishida, J. Sakata, *J. Am. Chem. Soc.* **1981**, *103*, 2106–2108; c) R. Noyori, I. Nishida, J. Sakata, *J. Am. Chem. Soc.* **1983**, *105*, 1598–1608.

[21] C. Chuit, R. Corriu, C. Reye, *J. Organomet. Chem.* **1988**, *358*, 57.

[22] a) C. Gennari, M. Beretta, A. Bernardi, G. Moro, C. Scolastico, R. Todeschini, *Tetrahedron* **1986**, *42*, 893–909; b) C. Gennari, A. Bernardi, S. Cardani, C. Scolastico, *Tetrahedron Lett.* **1985**, *26*, 797–800.

[23] a) V. Gutmann, *The Donor–Acceptor Approach to Molecular Interactions*, Plenum Press, New York, **1978**; b) W. Jensen, *The Lewis Acid–Base Concept*, Wiley Interscience, New York, **1980**.

[24] R. Noyori, S. Murata, M. Suzuki, *Tetrahedron* **1981**, *37*, 3899–3910.

[25] a) S. E. Denmark, B. R. Henke, *J. Am. Chem. Soc.* **1991**, *113*, 2177; b) S. E. Denmark, W. Lee, *Tetrahedron Lett.* **1992**, *33*, 7729–7732; c) S. E. Denmark, W. Lee, *J. Org. Chem.* **1994**, *59*, 707–709; d) B. Henke, PhD thesis, University of Illinois (Urbana-Champaign), **1989**.

[26] S. L. Schreiber, J. A. Reagan, *Tetrahedron Lett.* **1986**, *27*, 2945–2948.

[27] The proposal that the dioxolanone is attacked first is supported by the observation that with 1 equivalent of DIBALH, aldehyde **3** was recovered in high yield after acid workup.

[28] a) A. Mancuso, S.-L. Huang, D. Swern, *J. Org. Chem.* **1978**, *43*, 2480–2482; b) A. Mancuso, D. Swern, *Synthesis* **1981**, *1981*, 165–185; c) T. Tidwell, *Synthesis* **1990**, *1990*, 857–870.

[29] The configurational assignments of the two diastereomers were made on the basis of a previous study in which these compounds were unambiguously assigned.[25]

[30] a) D. Cox, J. Terpinski, W. Lawrynowicz, *J. Org. Chem.* **1984**, *49*, 3216; b) R. Sharma, J. Fry, *J. Org. Chem.* **1983**, *48*, 2112–2114.

[31] T. Chan, T. Aida, P. Lau, V. Groys, D. Harpp, *Tetrahedron Lett.* **1979**, *20*, 4029–4032.

[32] G. Helmchen, U. Leikauf, I. Taufer-Knöpfel, *Angew. Chem.* **1985**, *97*, 874–876; *Angew. Chem. Int. Ed. Engl.* **1985**, *24*, 874–875.

[33] J. Donaldson, *Prog. Inorg. Chem.* **1967**, *8*, 287–356.

[34] a) E. Hough, D. Nicholson, *J. Chem. Soc. Dalton Trans.* **1976**, 1782–1785; b) R. Andrews, J. Donaldson, D. Nicholson, *Acta Crystallogr. Sect. B* **1977**, *33*, 307–308.

[35] a) H. Kiriyama, K. Kitahama, O. Nakamura, R. Kiriyama, *Bull. Chem. Soc. Jpn.* **1973**, *46*, 1389–1395; b) P. Ewings, P. Harisson, T. King, *J. Chem. Soc. Dalton Trans.* **1975**, 1455.

[36] H. Gilman, F. Schulze, *J. Am. Chem. Soc.* **1925**, *47*, 2002–2005.

[37] H. Brown, N. Ravindran, *Inorg. Chem.* **1977**, *16*, 2938–2940.